

# Preparation and performance of a Cu–CeO<sub>2</sub>–ScSZ composite anode for SOFCs running on ethanol fuel

Xiao-Feng Ye<sup>\*</sup>, Bo Huang<sup>\*\*</sup>, S.R. Wang, Z.R. Wang, L. Xiong, T.L. Wen

*Shanghai Institute of Ceramics, Chinese Academy of Sciences (SICCAS), 1295 Dingxi Road, Shanghai 200050, PR China*

Received 8 September 2006; received in revised form 17 October 2006; accepted 18 October 2006

Available online 27 November 2006

## Abstract

Solid oxide fuel cells (SOFCs) that can operate directly on hydrocarbon fuels, without external reforming, have the potential of greatly speeding up the application of SOFCs for transportation and distributed-power supplies. In this paper, a dual tape casting method for fabricating an anode-supported thin-electrolyte (scandia stabilized zirconia (ScSZ)) film and SOFCs that are active for the oxidation of wet ethanol was presented. The fabrication method relies upon the inclusion of ammonium oxalate ((NH<sub>4</sub>)<sub>2</sub>C<sub>2</sub>O<sub>4</sub>·H<sub>2</sub>O) pore formers in the anode green tape in order to produce a porous ScSZ matrix, which forms the anode after wet impregnation with aqueous solutions of Cu(NO<sub>3</sub>)<sub>2</sub> and Ce(NO<sub>3</sub>)<sub>3</sub>, and firing. Anodes with different ratios of copper to ceria but with the same total loading were fabricated and measured. The performance characteristics for such cells were studied in both H<sub>2</sub> and C<sub>2</sub>H<sub>5</sub>OH + H<sub>2</sub>O, for comparison, and the long-term performance of the cells in C<sub>2</sub>H<sub>5</sub>OH stream at 800 °C was also presented. © 2006 Elsevier B.V. All rights reserved.

**Keywords:** Solid oxide fuel cell (SOFC); Direct internal reforming; Scandia stabilized zirconia; Composite anode; Ethanol; Carbon deposition

## 1. Introduction

Due to their high efficiencies, low cost and fuel flexibility, solid oxide fuel cells (SOFCs) are considered to be promising candidates for electrical power generation. Many fuels have been suggested as potentially applicable to SOFCs and among them, ethanol is considered to be an attractive “green” fuel due to the following reasons: ethanol is a liquid fuel which is easy and safe in storage, handling and delivery; ethanol is renewable from various biomass sources including energy plants, waste materials from agriculture, forestry residue materials and even organic fractions from solid wastes; ethanol can be easily mixed with the necessary amount of water and vaporized simultaneously for reforming; ethanol nowadays is widely available and there seems to be no difficulty in its supply infrastructure.

It is well known that Ni–YSZ (yttria stabilized zirconia) cermet anodes of solid oxide fuel cell have excellent catalytic properties and stability for the H<sub>2</sub> oxidation at SOFC opera-

tion conditions [1,2]. However, since Ni is a good catalyst for the hydrocarbon cracking reaction, the use of hydrocarbon fuels in an SOFC with Ni-based anode results in carbon deposition and rapid, irreversible cell degradation [3–7]. Ni–YSZ cermet anodes can only be directly used for hydrocarbon fuels if excess steam is present to ensure complete fuel reforming and to suppress carbon deposition [4,8].

Gorte and his co-workers focused their attention on developing carbon resistant anodes by replacing Ni with Cu and CeO<sub>2</sub> [9–13]. Compared to Ni, Cu is not catalytically active for carbon deposition but is effective as a current collector, while ceria provides a high catalytic activity for hydrocarbon reforming due to its special mixed conductivity. Since the melting points of both copper and copper oxide are significantly less than the sintering temperature of, ca. 1500 °C which is necessary for the densification of electrolytes, it is not possible to prepare Cu–YSZ cermets by high temperature sintering technology. Therefore, an alternative method for preparing Cu–YSZ cermets was developed in which a porous YSZ matrix was prepared first, and then both Cu and CeO<sub>2</sub> were added through wet impregnation [10,12].

In this paper, we present a tape casting method for preparing SOFCs with a Cu–CeO<sub>2</sub>–ScSZ anode, and study the cells’ performance in ethanol with steam for a long time. Tape casting is favorable for preparing very thin electrolyte films, and

<sup>\*</sup> Corresponding author. Tel.: +86 21 52412058; fax: +86 21 52413903.

<sup>\*\*</sup> Corresponding author.

*E-mail addresses:* [yexf@mail.sic.ac.cn](mailto:yexf@mail.sic.ac.cn) (X.-F. Ye), [huangbo2k@hotmail.com](mailto:huangbo2k@hotmail.com) (B. Huang).

multi-layer structures. It is also easy in scaling up. We adopted this process to prepare a thin dense film of scandia stabilized zirconia (ScSZ) electrolyte, supported by a thick porous ScSZ layer which serves as the framework for the final anode. Ammonium oxalate ( $(\text{NH}_4)_2\text{C}_2\text{O}_4 \cdot \text{H}_2\text{O}$ ) was used as the pore former. Although wet impregnation of Cu and  $\text{CeO}_2$  was carried out with a similar process as in the YSZ system [10,12], the method adopted in this study is able to prepare large area cells, which are necessary for real application of SOFCs. In previous work, on Cu– $\text{CeO}_2$ –YSZ composite anodes by others, the ratios of Cu: $\text{CeO}_2$  were not stable, so the influence was not clear. In order to study the influence of different amounts of copper and ceria on the fuel oxidation, we fabricated, measured and compared anodes with different ratios of copper to ceria. We also demonstrated the feasibility and stability of using liquid fuels such as ethanol on Cu– $\text{CeO}_2$ –ScSZ composite anodes.

## 2. Experimental

### 2.1. Preparation of porous anode matrix

Fine ScSZ powders (99.99% pure, Daiichi Kigenso, Japan) and ammonium oxalate reagent (99.8% pure) were used to prepare the porous supporter of ScSZ by a tape casting and subsequent sintering process. The solvent system used in this paper was an azeotropic mixture of butanone and ethyl alcohol. Triethanolamine as a kind of zwitterionic dispersant was used as the dispersant. Poly-vinyl-butyl (PVB) and a mixture of polyethylene glycol (PEG 200) and dibutyl-*o*-phthalate (DOP) were used as the binder and plasticizer, respectively. All the organic additives were supplied by Shanghai Chem. Ltd., China.

The amount of ammonium oxalate pore formers (200 mesh) ranged from 10 to 60 wt.% in the ScSZ powders. Starting materials were weighed, mixed and ball milled, then a homogeneous slurry was obtained. The slurry was degassed using a vacuum pump (pressure: 200 mbar absolute) and cast onto a glass surface. The green tapes were allowed to dry at room temperature for 48 h. They were then sintered in air at 1450 °C for 3 h. The porosities of the sintered porous ScSZ layers were determined using a standard test method based on Archimedes' principle by measuring the mass of water that could be absorbed into the porous ScSZ layer [15]. The microstructure of the sintered porous ScSZ layer before and after impregnation was analyzed by scanning electron microscope (SEM) images using a microscope (SEM, PHILIPS 515, Holland) equipped with an X-ray analyzer for energy-dispersive X-ray spectroscopy (EDS).

### 2.2. Fabrication of unit-cells

Anode-supported SOFCs were fabricated using dual tape cast layers of ScSZ, one containing pore formers (the porous anode matrix) and the other without pore formers (the electrolyte layer). The electrolyte layer was cast first and then allowed to dry at room temperature for 48 h. A second layer of ScSZ which contained pore formers was then cast on top of the electrolyte

green tape and allowed to dry overnight. The composite structure was then sintered in the air at 1450 °C for 3 h. The cathode with 1.54 cm<sup>2</sup> area was fabricated by screen-printing a slurry containing  $(\text{Pr}_{0.7}\text{Ca}_{0.3})_{0.9}\text{MnO}_3$  (provided by co-workers in our lab) onto the surface of the dense ScSZ electrolyte and then sintered at 1200 °C for 3 h. SEM images showed that the thickness of the dense ScSZ layer, porous ScSZ layer and PCM cathode of the single cell used in this study were about 20, 600 and 30 μm, respectively.

### 2.3. Cu– $\text{CeO}_2$ coating

The Cu– $\text{CeO}_2$ –ScSZ anodes were prepared by impregnating the porous ScSZ layer with aqueous solutions of  $\text{Cu}(\text{NO}_3)_2 \cdot 3\text{H}_2\text{O}$  and  $\text{Ce}(\text{NO}_3)_3 \cdot 6\text{H}_2\text{O}$  into the anode matrix, followed by low temperature calcinations at 450 °C to form the oxides. The calcination temperature of  $\text{Cu}(\text{NO}_3)_2 \cdot 3\text{H}_2\text{O}$  and  $\text{Ce}(\text{NO}_3)_3 \cdot 6\text{H}_2\text{O}$  were determined from their TG curves. Anodes with different ratio of copper versus ceria were fabricated by impregnating solutions containing different amount of  $\text{Cu}(\text{NO}_3)_2$  and  $\text{Ce}(\text{NO}_3)_3$ . For these cells the total amount of Cu and  $\text{CeO}_2$  was held constant at 30 wt.%, while the ratio of Cu to  $\text{CeO}_2$  in the anode was varied. The impregnated Cu and  $\text{CeO}_2$  weight loading in the ScSZ anode matrix was calculated from the weight change of the ScSZ anode matrix before and after the impregnation treatment. We made four kinds of cells with different ratios of 2.5:1 (21.5 wt.% Cu–8.5 wt.%  $\text{CeO}_2$ , denoted as cell 1), 2:1 (20 wt.% Cu–10 wt.%  $\text{CeO}_2$ , denoted as cell 2), 1.5:1 (18 wt.% Cu–12 wt.%  $\text{CeO}_2$ , denoted as cell 3) and 1:1 (15 wt.% Cu–15 wt.%  $\text{CeO}_2$ , denoted as cell 4).

### 2.4. Characterization of single cell performance

SOFC tests were carried out in a single cell test setup, which is illustrated in Fig. 1. A Pt mesh and Au lead wire as the current collector were attached to the surface of the anode and cathode using a Pt paste. The cathode side of the structure was then attached to an alumina tube using Pt paste and the edges were sealed using a glass ring. All the anodes were evaluated with the same testing procedure. The anodes were fully reduced in a

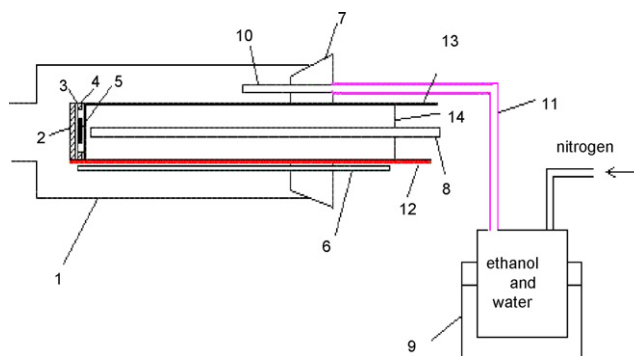


Fig. 1. Schematic drawing of cell test set up. (1) Furnace tube, (2) anode, (3) electrolyte, (4) glass seal, (5) cathode, (6) thermocouple, (7) seal plug, (8) oxygen inlet, (9) water bath, (10) fuel inlet, (11) heating tape and copper tube, (12) anode lead wire, (13) cathode lead wire, (14) alumina tube.

H<sub>2</sub> atmosphere at 800 °C for several hours prior to cell testing. In order to avoid copper sintering and to keep the anode performance, the measurement was carried out in the temperature range of 700–800 °C with an interval of 50 °C.

Hydrogen or gasified ethanol–water mixture (with volume ratio 2:1) were used as fuel and oxygen was used as oxidant. The fuel and oxidant flow rate were all controlled at 25 mL min<sup>-1</sup>, and the liquid fuel was vaporized by water bath (70 °C) and then brought into the anode surface by nitrogen. The current–voltage curves and electrochemical impedance spectroscopy (EIS) were obtained using an Electrochemical Workstation (IM6, ZAHNER). The impedance spectra of the electrochemical cell were recorded at open circuit voltage (OCV) with amplitude of 20 mV over the frequency range 0.02 Hz–100 KHz.

### 3. Results and discussion

#### 3.1. Microstructural characterization

##### 3.1.1. Porous anode matrix characterization

The effect of the amount of pore formers on the porosity of the anode film was initially studied. The porosity, defined as the void volume divided by the total volume of the sintered anode film, is plotted in Fig. 2 as a function of the weight percent of pore formers in the green tape. It is noted that the weight percent of pore formers is based on the mass of ScSZ powders in the green tape. We can find that the porosity of the sintered porous ScSZ layer increases linearly with the weight percent of pore formers up to 40 wt.%. Further increase in the weight percent of pore formers did not have a significant effect on the porosity of the sintered porous ScSZ layer. The data in Fig. 2 also shows that decreasing the sintering temperature from 1450 °C to 1400 °C had little effect on the porosity of the sintered p-ScSZ layer.

Fig. 2 also shows the linear shrinkage as a function of weight percent of pore formers in the porous ScSZ green tapes. The figure shows that the linear shrinkage was all in the vicinity

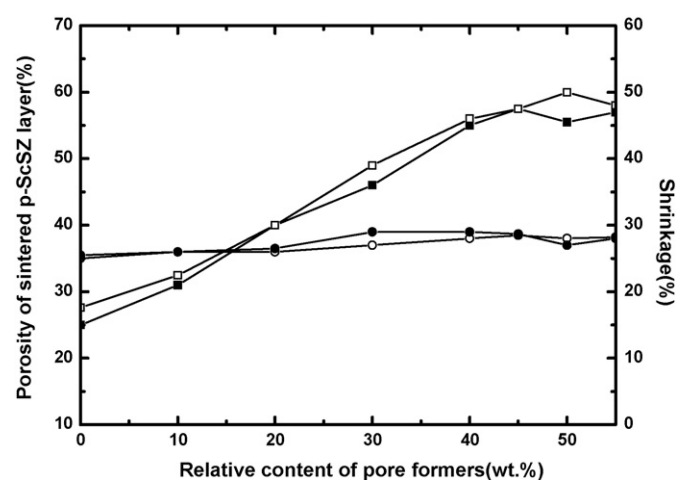


Fig. 2. Porosity (■) and linear shrinkage (●) of samples sintered at 1400 °C (open) and 1450 °C (closed) as a function of weight percent of pore formers in green porous ScSZ tape.

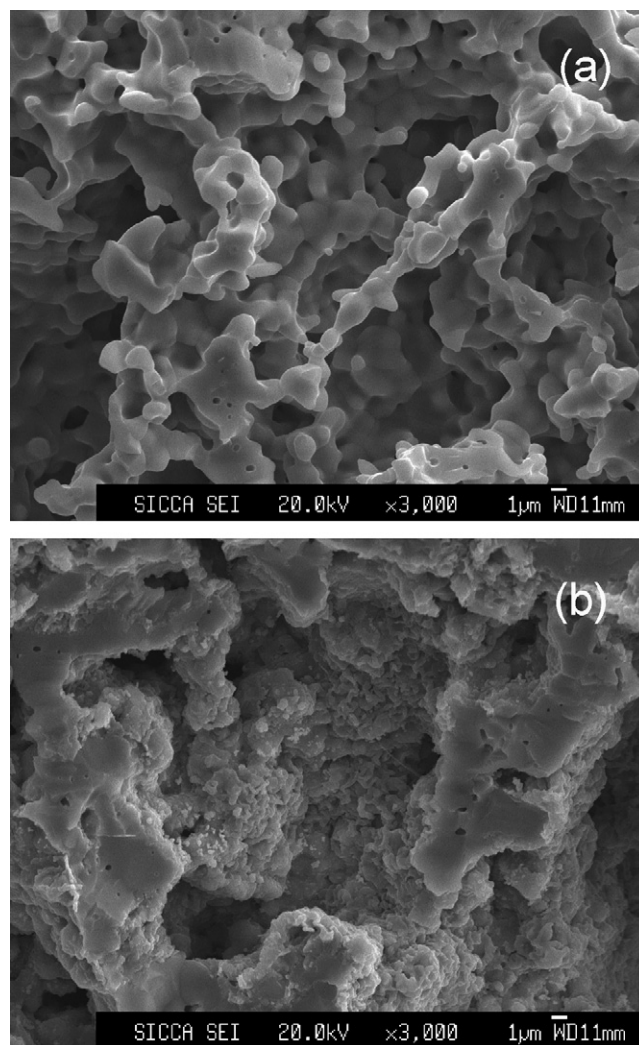


Fig. 3. SEM images of the porous anode matrix: (a) before impregnation; (b) after 50 h operation.

of 27% and independent of the amount of pore formers in the green tapes. It is noted that there was not a significant difference between the shrinkage for ScSZ tapes without pore formers and those with pore formers. Therefore, it is possible to fabricate a green ScSZ tape with pore formers on one side, and supporting the other side without pore formers and to co-sinter them without introducing undue stress or cracks in either layer.

##### 3.1.2. SEM characterization

The microstructure of an anode has a great effect on the performance of the SOFC because the electrochemical reactions of the fuel cells take place mainly at the triple phase boundaries (TPB), where the reaction gas meets the electrode and electrolyte. Fig. 3 shows the cross-sectional SEM micrographs of porous ScSZ anode matrix before impregnation (a) and after cell operation (Cu/CeO<sub>2</sub> 2.5) (b). For this cell, the p-ScSZ green tape contained 40wt.% ammonium oxalate and was ca.55% porous after sintering. The micrographs show that the morphology of the porous ScSZ layer is relatively uniform with pores of average size about 20 μm, which suggests that the pore formers

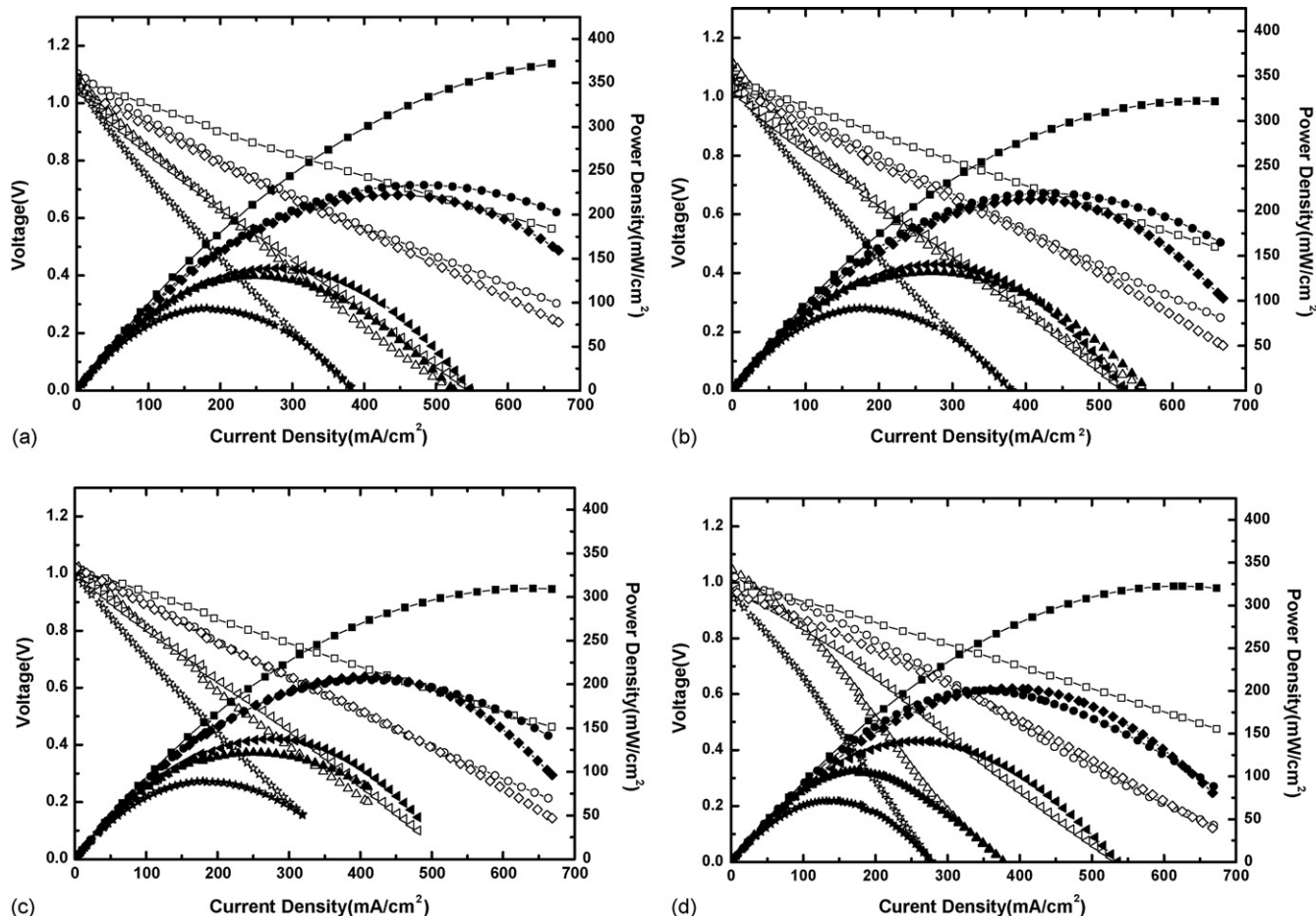


Fig. 4. Voltage (open) and power density (closed) vs. current density while running on  $\text{H}_2$  at  $800^\circ\text{C}$  (■),  $750^\circ\text{C}$  (●),  $700^\circ\text{C}$  (▲), and  $\text{C}_2\text{H}_5\text{OH} + \text{H}_2\text{O}$  at  $800^\circ\text{C}$  (□),  $750^\circ\text{C}$  (◀),  $700^\circ\text{C}$ , (★) for cell 1(a), cell 2(b), cell 3(c) and cell 4(d).

are homogeneously distributed throughout the tape prior to sintering. After impregnation, we can see well-connected copper and ceria films formed on the framework of the ScSZ matrix.

### 3.2. Performances of single cells

Fig. 4 shows curves of voltage and power density versus current density while running on humidified hydrogen and ethanol stream at  $800^\circ\text{C}$ ,  $750^\circ\text{C}$  and  $700^\circ\text{C}$  for cell 1(a), cell 2(b), cell 3(c) and cell 4(d). We can see that the open circuit voltages (OCV) for  $\text{H}_2$  and  $\text{C}_2\text{H}_5\text{OH}$  were respectively, 1.02–1.12 V and 0.98–1.1 V in the temperature range, which were all slightly below the theoretical OCVs. It reveals that ScSZ electrolyte was not dense enough that resulted in decreased values of OCV.

In Fig. 5 while using hydrogen as fuel, shows the maximum power density for cell 1 at  $800^\circ\text{C}$ ,  $750^\circ\text{C}$  and  $700^\circ\text{C}$ , respectively reached  $372$ ,  $234$  and  $130 \text{ mW cm}^{-2}$ , respectively, whereas the corresponding values for cells 2, 3 and 4 were  $322$ ,  $220$ ,  $122 \text{ mW cm}^{-2}$ ,  $310$ ,  $205$ ,  $122 \text{ mW cm}^{-2}$  and  $323$ ,  $201$ ,  $106 \text{ mW cm}^{-2}$ , respectively. At the same temperature, the values decreased from cell 1 to cell 4 with decreasing copper amounts. While operating on ethanol stream, the maximum power density

of cell 1 was  $222$ ,  $139$  and  $94 \text{ mW cm}^{-2}$  at  $800^\circ\text{C}$ ,  $750^\circ\text{C}$  and  $700^\circ\text{C}$ , respectively, which were lower than with hydrogen, and we can also see the same decreasing tendency of the four cell performances.

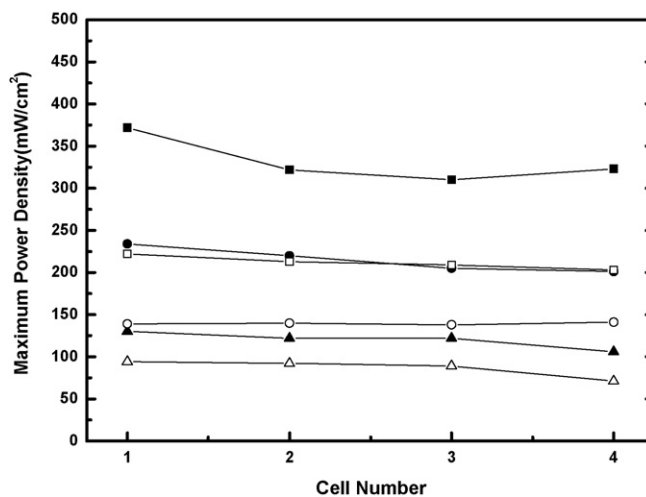


Fig. 5. Maximum power density for cell 1, cell 2, cell 3 and cell 4 while running on  $\text{H}_2$  (closed) and  $\text{C}_2\text{H}_5\text{OH} + \text{H}_2\text{O}$  (open) at  $800^\circ\text{C}$  (■),  $750^\circ\text{C}$  (●) and  $700^\circ\text{C}$  (▲).

It is known that in Cu–CeO<sub>2</sub>–ScSZ anode, ceria is a catalyst for fuel oxidation, while copper provides the conductive path of electrons in the anode. From cell 1 to cell 4, the cell performance decreased with decreasing copper amounts while the total loading was kept the same. As a catalyst, ceria addition is critical, however, when the amount of ceria in the anode reached some value, further increases in ceria amount had no effect on cell performance, while increases in copper provided a better conductive network, to improve the cell performance. So in the four cells, cell 1 showed the best performance in both hydrogen and ethanol steam. Also we can include that at 800 °C and 750 °C the cell performances are almost the same as the results seen before [14], however, the cell performance at 700 °C is poor compared to them. With a decrease in temperature, cell performance decreased. It has been revealed that cathode polarization contributed the most to cells' internal resistance, so the poor performance of the cells would be improved if the PCM cathode is replaced by a better one.

In an attempt to examine the reason for the different cell performances in Fig. 6, we measured the impedance spectra of cell 1–4 while running on H<sub>2</sub> (a), and C<sub>2</sub>H<sub>5</sub>OH + H<sub>2</sub>O (b) at 800 °C. The ohmic resistance,  $R_{\Omega}$ , is the real-axis intercept at high frequency.  $R_{\Omega}$  for cell 1–4 at 800 °C are respectively 0.29, 0.31, 0.42 and 0.46  $\Omega \text{ cm}^2$ , which almost kept the same as the values for ethanol, and the ohmic resistance of the cells increased from cell 1 to cell 4 because of lower copper content. The total resistance of the cell,  $R_t$ , is the real-axis intercept at low frequency. In Fig. 6 we can also see  $R_t$  increases from cell 1 to cell 4, and it shows the same tendency for both hydrogen and ethanol steam. The tendency also confirms that cell 1 shows the best performance in the four cells.

A detailed study of anode-supported cells running on hydrogen has shown that cell power densities can be limited by a number of factors, including concentration polarization [15,16]. The decrease in cell power density for ethanol stream relative to hydrogen may be related to the higher mass of ethanol molecules, which yields slower gas-phase diffusion and increased concentration polarization. However, it is also noted that each ethanol molecule reacts with six times as many oxygen ions as each hydrogen molecule, so less ethanol gas-phase diffusion is needed to yield the same cell current density. Another possible explanation is the difference in the nature of the oxidizing and reducing species, which makes the charge transfer in ethanol more complex and difficult. H<sub>2</sub> is obviously more active and more effective for reduction. C<sub>2</sub>H<sub>5</sub>OH is much less reactive than H<sub>2</sub> in heterogeneous oxidation, thus, resulting in a higher polarization resistance associated with slower electrochemical oxidation of ethanol versus hydrogen. So the steps and mechanism of ethanol oxidation need to be studied later by analyzing the components of the fuel effluent in order to improve the Cu–CeO<sub>2</sub>–ScSZ composite anode performance for hydrocarbons.

### 3.3. Long-term performances

To gain information on the cell long-term performance and carbon formation, we kept every cell discharging at 0.5 V for

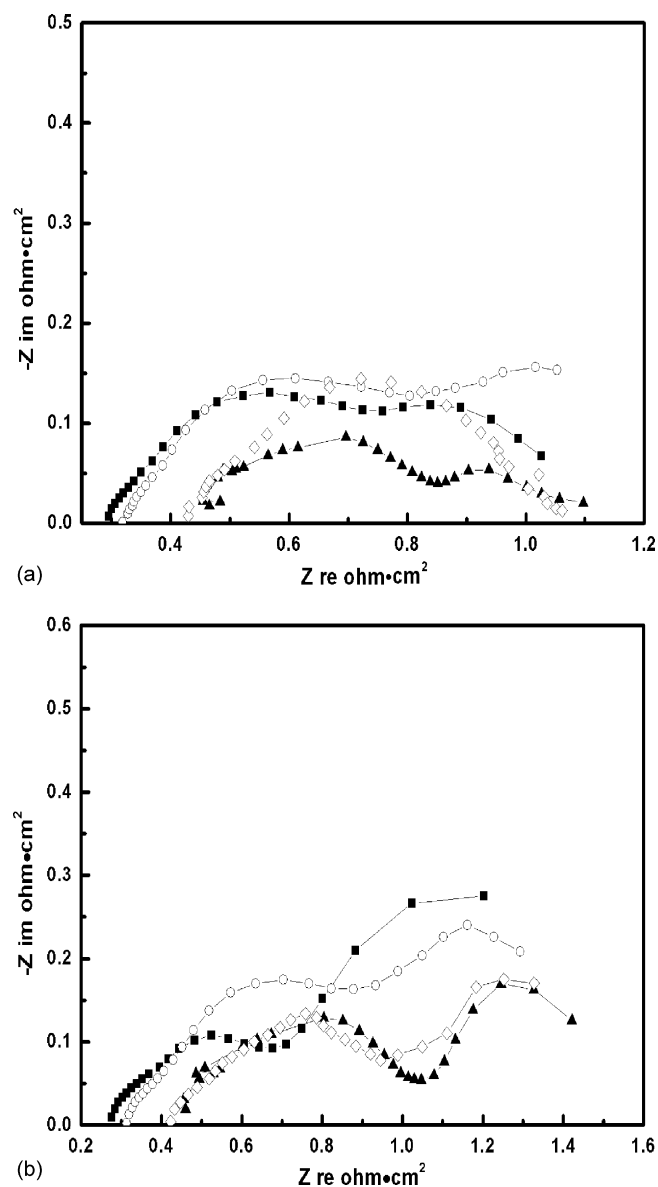


Fig. 6. Impedance spectra for cell 1(■), cell 2(○), cell 3(◇) and cell 4(▲) while running on H<sub>2</sub> (a), and C<sub>2</sub>H<sub>5</sub>OH + H<sub>2</sub>O (b) at 800 °C.

at least 5 h, cell 2 specially for 50 h, and recorded the curve of power density as a function of time for the four cells operating on ethanol steam at 800 °C. From Fig. 7 we know that in the time period, all the cells performance almost kept constant with a little increase of power density with time. The small fluctuation of power density may be partly attributed to the unstable ethanol flow by our method. In Fig. 8 we see that for a longer time of 50 h, the cell performance still kept constant without any degradation. After 50 h of operation, the anode surface was dark red and a little carbon had deposited on the anode surface, so we think that the Cu–CeO<sub>2</sub>–ScSZ composite anode performance kept constant while operating on hydrocarbons. We also concluded from Fig. 9 that the ohmic resistance of the cell increased with time from 0.31 to 0.56  $\Omega \text{ cm}^2$ . This phenomenon may be due to the poor combination of copper and

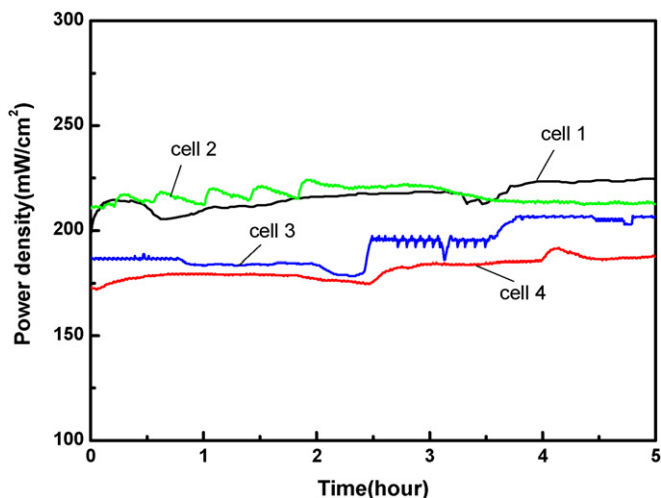


Fig. 7. Power density at 0.5 V as a function of time for cell 1 (black), cell 2 (green), cell 3 (blue) and cell 4 (red) operating on steam of ethanol and water, at 800 °C.

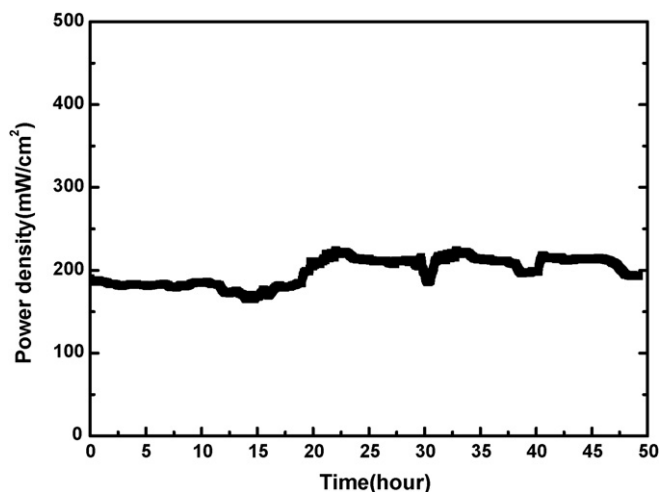


Fig. 8. Power density at 0.5 V as a function of time for cell 2 operating on the steam of ethanol and water, at 800 °C.

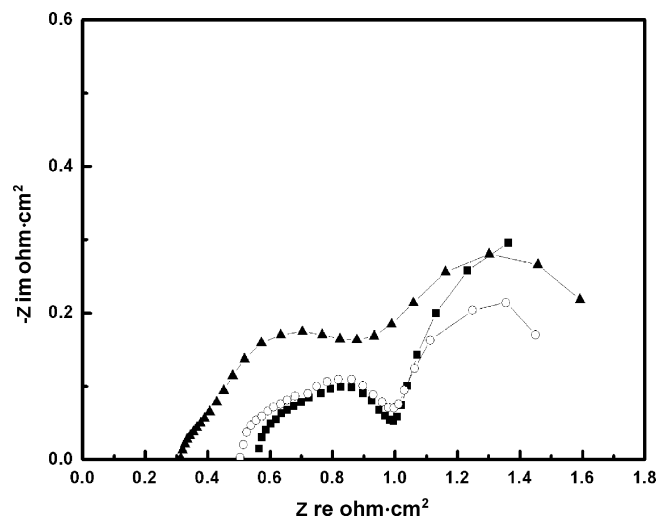


Fig. 9. Impedance spectra for cell 2 as a function of operation time: (▲) at the beginning; (○) after 20 h; (■) after 50 h.

the anode matrix because of the low calcination temperature, which resulted in mass transfer and related morphological changes of copper during cell operation. What is more interesting is that the polarization resistance and the total resistance decreased with time. Probably, the carbon particles, which deposited in the pores lead to better connections of the copper particles and much longer TPBs [10,17] which decreased the polarization resistance. We can also see that the total resistance of the cell didn't change a lot after 50 h of operation compared to 20 h, which proved the cell performance tended to be stable.

#### 4. Conclusions

We successfully fabricated a Cu–CeO<sub>2</sub>–ScSZ composite anode by impregnating solutions of copper and cerium nitrates into a porous ScSZ matrix made by a tape casting method and we also produced unit cells with different ratio of copper versus ceria, of which cell 1 with 21.5 wt.% Cu–8.5 wt.% CeO<sub>2</sub>–ScSZ anode showed the best performance. The cell performances were good while using H<sub>2</sub>, C<sub>2</sub>H<sub>5</sub>OH + H<sub>2</sub>O as fuels at 800 °C and 750 °C, but poor at 700 °C partly due to the poor cathode performance. The Cu–CeO<sub>2</sub>–ScSZ composite anode showed a good and stable performance for hydrocarbons, after 50 h of operation on ethanol steam, the cell performance almost kept the same with power density at 210 mWcm<sup>-2</sup> and there was no visible carbon deposition on the anode surface after operation, but the steps and mechanism of ethanol oxidation need to be studied more by analyzing the components of the fuel effluent in order to improve the Cu–CeO<sub>2</sub>–ScSZ composite anode performance for hydrocarbons.

#### Acknowledgements

The authors thank the financial support from Chinese Government High Tech Developing Project (2003AA517010) and the Postdoctoral Foundation of Shanghai (Grant No. 06R214156), and also thank Lin Xiong for providing PCM powders.

#### References

- [1] S.P. Jiang, S.H. Chan, *Mater. Sci. Technol.* 20 (2004) 1109–1118.
- [2] S.P. Jiang, S.H. Chan, *J. Mater. Sci.* 39 (2004) 4405–4439.
- [3] C.H. Bartholomew, *Catal. Rev. Sci. Eng.* 24 (1982) 67–70.
- [4] R.T.K. Baker, *Carbon* 27 (1989) 315–323.
- [5] B.C.H. Steele, *Solid State Ionics* 86–88 (1996) 1223–1234.
- [6] K. Hernadi, A. Fonseca, J.B. Nagy, A. Siska, I. Kiricsi, *Appl. Catal. A* 199 (2000) 245–255.
- [7] J.H. Koh, Y.-S. Yoo, J.-W. Park, H.C. Lim, *Solid State Ionics* 149 (2002) 157–166.
- [8] R.J. Farrauto, C.H. Bartholomew, *Fundamentals of Industrial Catalytic Processes*, 1st ed., Blackie Academic & Professional, London, 1997, pp. 341–343.
- [9] S. Park, J.M. Vohs, R.J. Gorte, *Nature (Lond.)* 404 (2000) 265–266.
- [10] R.J. Gorte, S. Park, J.M. Vohs, C. Wang, *Adv. Mater.* 12 (2000) 1465–1469.
- [11] S. Park, R. Craciun, J.M. Vohs, R.J. Gorte, *J. Electrochem. Soc.* 146 (1999) 3603–3605.

- [12] S. Park, R.J. Gorte, J.M. Vohs, J. Electrochem. Soc. 148 (2001) A443–A447.
- [13] H. Kim, C. da Rosa, M. Boaro, J.M. Vohs, R.J. Gorte, J. Am. Ceram. Soc. 85 (2002) 1473–1476.
- [14] R. Farrauto, M. Hobson, T. Kennelly, E. Waterman, Appl. Catal. A81 (1992) 227–237.
- [15] S. de Souza, S.J. Visco, L.C. De Jonghe, J. Electrochem. Soc. 144 (1997) L35–L37.
- [16] J.W. Kim, A.V. Virkar, K.Z. Fung, K. Mehta, S.C. Singhal, J. Electrochem. Soc. 146 (1) (1999) 69–78.
- [17] H. Kim, C. Lu, W.L. Worrel, J.M. Vohs, R.J. Gorte, J. Electrochem. Soc. 149 (2002) A247–A250.